Meteorologische Zeitschrift, Vol. **14**, No. 6, 703-710 (December 2005)

Article

Time series of freshwater-transport on the East Greenland Shelf at 74°N

JÜRGEN HOLFORT[1] and JENS MEINCKE*[2]

[1]Norsk Polarinstitutt, Tromsø, Norway
[2]Universität Hamburg, Institut für Meereskunde, Hamburg, Germany

(Manuscript received February 7, 2005; in revised form August 8, 2005; accepted October 10, 2005)

Abstract

The major flux of freshwater from the Arctic Ocean to the convective regions in the Nordic Seas and the Northern North Atlantic is linked to the shelf branches of the East Greenland Current. This flux is partitioned into a solid (ice) and a liquid phase. Time series measurements of the liquid component are hard to obtain since the seasonally varying ice cover prevents the use of standard moored instrumentation in the near surface gradient layers where most of the freshwater transport takes place. Using 40m-polyethylene tubes to protect sensors and buoyancy in the upper portion of the moorings and employing a bottom-mounted acoustic Doppler current profiler have yielded the first time series of upper layer temperatures, salinities and currents for a location at the outer East Greenland shelf at 74°N. The observed seasonal variability suggests the dominance of local warming/cooling and melting/freezing rather than advective processes. Estimates of liquid freshwater transport yield a mean of 869 km^3/a, whereas the total freshwater transport amounts to a value between 1250 to 1750 km^3/a.

Zusammenfassung

Der Transport von Süßwasser aus dem Arktischen Ozean in die konvektiven Wirbel der Grönland-, Island- und Labradorsee erfolgt im Ostgrönlandstrom. Er besteht aus zeitlich veränderlichen Anteilen in fester (Eis) und flüssiger Form. Zeitreihenmessungen des flüssigen Süßwasseranteiles sind schwierig zu erhalten, da die saisonal veränderliche Eisbedeckung des Ostgrönlandstromes den Einsatz verankerter Sensoren in Oberflächennähe, dort wo sich der stärkste vertikale Gradient des Salzgehaltes befindet, sehr risikoreich macht. Durch die Verwendung von 40 m langen Polyäthylenrohren, in denen die Temperatur- und Salzgehaltssensoren sowie die Auftriebselemente des oberen Teiles der Verankerungskette untergebracht wurden, konnten erstmals 3-jährige Zeitreihen (2000–2003) der Schichtung des Ostgrönlandstromes auf dem ostgrönländischen Schelf bei 74°N erhalten werden. Die für Transportabschätzungen notwendigen Strömungsmessungen wurden durch den Einsatz eines am Grund verankerten, akustischen Doppler-Profilstrommessers gewonnen (2001–2002). Die beobachteten Jahresgänge von Temperatur und Salzgehalt werden durch lokale Erwärmung/Abkühlung bzw. Schmelzen/Gefrieren dominiert. Der flüssige Süßwassertransport für den Zeitraum 2001–2002 ergab sich zu 869 km^3/a, die Werte für den gesamten Süßwassertransport lagen im Bereich 1250 bis 1750 km^3/a.

1 Introduction

Freshwater export from the Arctic particularly affects stratification in the convective regions of the Northern North Atlantic and hence the Atlantic meridional overturning circulation.. For the Nordic Seas sector the export is facilitated by the polar components of the East Greenland Current (EGC), i.e. the Sea Ice, the Polar Surface Water and the Polar Intermediate Water (RUDELS et al., 2002). There is a definite gap in our knowledge about the partitioning of the freshwater flux into its solid and its liquid component along the path of the EGC from the Fram Strait to south of the Denmark Strait. Filling this gap is important since the processes and the time scales of freshwater supply to the sensitive convective gyres of the Greenland and the Iceland Seas are different for solid and liquid sources. Reliable data are needed since the last decades have seen important changes in the contribution of freshwater to the Nordic Seas watermass structure: There is the decadal freshening of the upper and intermediate waters and the related overflows (DICKSON et al., 2002; HANSEN et al., 2001), and there is the enhanced eastward penetration of freshwater within the Jan Mayen and the East Icelandic Currents into the Norwegian and the Lofoten Basins (BLINDHEIM et al., 2000).

The freshwater transport by ice through Fram Strait is sufficiently well measured and modeled. Transport values were estimated from Arctic water balances and local time series of ice thickness from upward looking sonars in combination with satellite measurements of ice speed and lateral ice extent. They range between 2360 and 2850 km^3/a (RUDELS, 1987; AA-

*Corresponding author: Jens Meincke, Universität Hamburg, Zentrum für Meeres- und Klimaforschung, Institut für Meereskunde, Bundesstr. 53, 20146 Hamburg, Germany, e-mail: meincke@ifm.uni-hamburg.de

0941-2948/2005/0079 $ 3.60

DOI: 10.1127/0941-2948/2005/0079

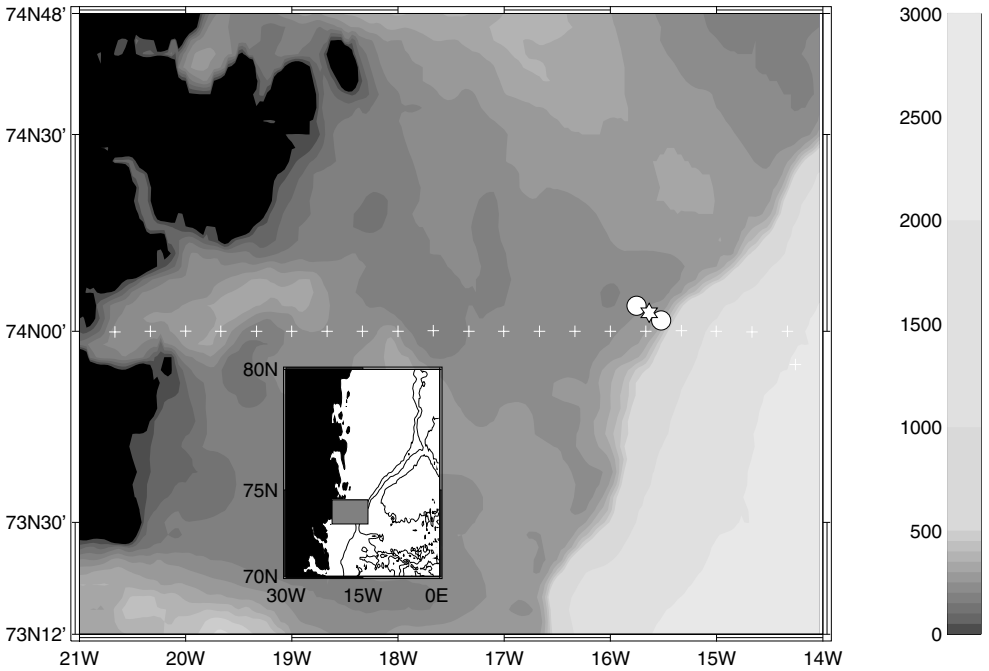

Figure 1: Map of the Greenland Shelf with mooring (circle=tube moorings, star=ADCP) and CTD (crosses) locations. Topographic contours are at every 50 m from 0 to 500 m and at 1000, 2000 and 3000 m.

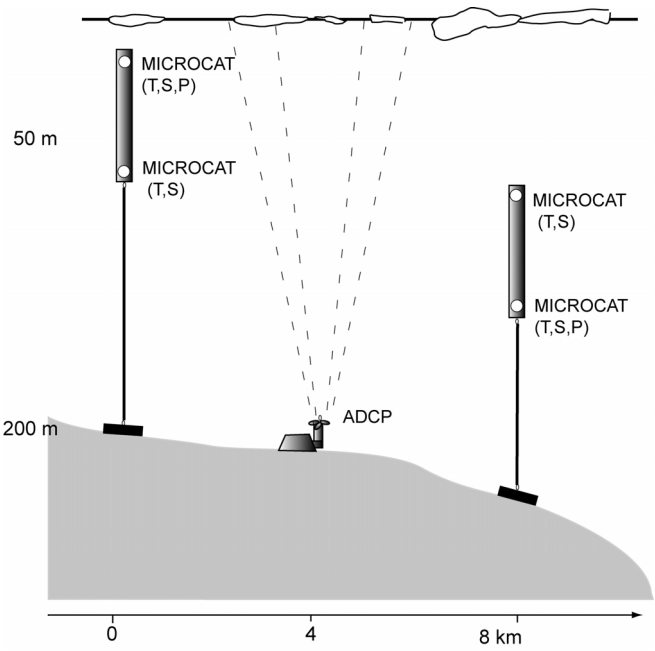

Figure 2: Schematic of the mooring deployment in 2001–2002.

GAARD and CARMACK, 1989; VINJE et al., 1998; and KWOK and ROTHROCK, 1999). Time series measurements and modeling show a variability up till 60 % of the annual means, with significant export anomalies in 1967/68 and in the 90´s (VINJE, 2001; HILMER et al., 1998; KOEBERLE and GERDES, 2003). From sensitivity experiments the low frequency variability in the wind forcing is the primary cause for the export variability (HAEKKINEN, 1999; HAAK et al., 2003).

In contrast to freshwater flux in the solid phase the liquid fluxes through Fram Strait have so far not been accessible to time series observations. Therefore numbers are mainly available from modeling and are given as 1600 km^3/a with anomalies on the order of 40 % of the mean (HAAK et al., 2003). AAGARD and CARMACK (1989) give an observation based estimate of 1160 km^3/a. Observations on the variability of the partitioning of the freshwater flux between the solid and the liquid phase are not available for Fram Strait and also not available for regions further downstream the EGC. The major reason for this shortcoming was the lack of adequate instrumentation for time series observations of currents and salinities throughout the watercolumn in the seasonally ice covered EGC over the East Greenland shelf and slope, including the sharp gradient layers immediately underneath the ice.

In a first attempt to obtain the required data we moored three instrument packages near the East Greenland shelf edge at 74°N (Figs.1 and 2). For measuring temperature and salinity as a function of depth, TS-recorders were mounted in a 40m-polyetylene tube which formed the upper buoyant end of a mooring. In case of contact with deeper reaching ice-keels or icebergs the rugged tube was supposed to be bent over without damage to the instruments and the bouyancy inside. For measuring the vertical current-distribution a bottom-mounted ADCP was deployed using traditional groundwire-technique. In this contribution we present TS-time series for the years 2001, 2002 and 2003 which will allow a first look at the seasonal variability of the

upper layers of the EGC. ADCP-data are only available for one year and will allow first measurement-based estimates of freshwater flux in the EGC for the period September 2001 to September 2002.

2 Measurements

Starting in September 2000, trial-moorings were placed on the east Greenland shelf at about 74°N to measure the near surface temperature and salinity stratification (Figs. 1 and 2, Tab. 1). The TS-sensors (Microcats, SBE 37 SM, recording interval 1 hour) were placed inside a 40 m long tube, including the flotation in the form of plastic spheres which fishermen use in trawling-nets. Near the instruments holes were drilled into the tube to facilitate water exchange. The tube was not filled evenly with flotation, rather we used more flotation in the lower part to ease tilting in case of ice contact. Due to the large cross section, the current drag on the tube is larger than in a normal mooring design and therefore more buoyancy is needed to prevent large vertical displacement due to strong currents. Calculations of the dynamic behavior (DEWEY, 1991) of a typical 200 m long mooring with a 40 m long tube on top gives a vertical displacement of about 22 m for a 0.5 m/s depth independent velocity (tube represented by a wire with 22 cm diameter, drag coefficient of 1.3 and 6.46 kg/m buoyancy). Increasing the buoyancy to 13 kg/m gives a vertical displacement of just 7 m. The measured (maximum of about 50 m) and calculated displacement for the 2001–2002 period show relatively good agreement. These calculations were possible because in the second year of deployment (9/2001 to 9/2002) an acoustic Doppler current profiler (ADCP) was moored on the bottom between the two tube moorings and measured the current in the whole water column. Pressure was not recorded in the first year of deployment, the following years the upper instrument of each tube recorded pressure. The pressure at the lower instrument was calculated from the upper one using the mooring tilt. Data within 10 dbar pressure bins was averaged into daily values, due to mooring tilt at some days therefore more depth bins than instruments are available. The bins around the nominal depths of 20 dbar and 60 dbar have one very few missing daily values. The ADCP made hourly measurements of the velocity in 11 vertical bins, covering the whole water column. It was mounted in a battom frame without releaser. At deployment this frame was lowered to the bottom with a wire of 300 m length. This wire was then stretched out on the ground with a weight at its end. At recovery we dredged for this wire and used it to recover the ADCP. In the design of the ADCP-frame the effect of its steel-weight on the ADCP-compass was underestimated. Therefore, in addition to correct the compass readings for the local magnetic variation using the International Geomagnetic Reference Field, we also had to account for a considerable magnetic deviation due to mooring frame and weight. This was done by assuming that the polar waters near the slope flow southward with their mean barotropic flow aligning with the direction of the regional scale depth contours (PROUDMAN, 1953). This direction was calculated by fitting a plane to the local topography ($\pm 1^\circ$ in longitude and $\pm 0.5^\circ$ in latitude). Depending on the topographic data that direction is -115° (Etopo2 from www.ngdc.noaa.gov) or -119° (IOC, IHO and BODC, 2003). We use the value of -119° and therefore had to apply a deviation of +29.5 degrees, resulting in a mean barotropic velocity of –6.8 cm/s northwards and -14.6 cm/s eastwards. The barotropic eddy kinetic energy ($\langle \bar{U}' \cdot \bar{U}' \rangle = 228\ \mathrm{cm}^2/\mathrm{s}^2$) with overbars denoting vertical and angle brackets temporal means is smaller than the mean kinetic energy ($\langle \bar{U} \rangle \cdot \langle \bar{U} \rangle = 260\ \mathrm{cm}^2/\mathrm{s}^2$). For the subsequent analysis the data was low pass filtered using a cutoff frequency of 28 hours to exclude the main tidal signal and averaged into daily means. This lowered the barotropic eddy kinetic energy to 155 $\mathrm{cm}^2/\mathrm{s}^2$. The direction of the barotropic current is quite stable, only 67 (42) out of 368 days the direction deviates more than 30 (45) degree from the mean direction. A smoothed time series of the velocity in the main direction is given in Fig. 4d. During the deployment and recovery cruises hydrographic sections were done using a Seabird 911+ CTD. In September 2001 and 2002 almost no ice was present at 74°N, so it was possible to obtain complete CTD sections for the shelf all the way to the coast of Greenland (Fig. 3). In September 2000 the ice edge was situated east of the shelf break. No CTD-profiles on the shelf are available from that summer.

3 Seasonal cycle

In Fig. 4 a,b and c we present the first 3-year time series of temperature and salinity for the upper layers of the outer shelf at 74°N. During spring and summer the ice formed in the preceding winter melts and the released freshwater lowers the salinity of the upper water column. The upper waters are also warmed, so that at the end of summer a relatively warm and fresh surface layer is present. As this layer is of lower density, a strong density contrast to the layer below inhibits mixing and exchanges between both layers. In autumn decreasing temperatures lower the density and ice formation increases the salinity in the surface layer. Mixing with the layer below leads to a quite homogeneous water column in winter, with temperatures near the freezing point. This cycle is clearly seen in the mooring data. The good correlation of the upper salinity with the local ice cover (correlation coefficient between monthly data $= +0.88$, and between daily data $= +0.84$) suggests that most of the changes are due to local processes of ice formation and melting, and that advection does not play a

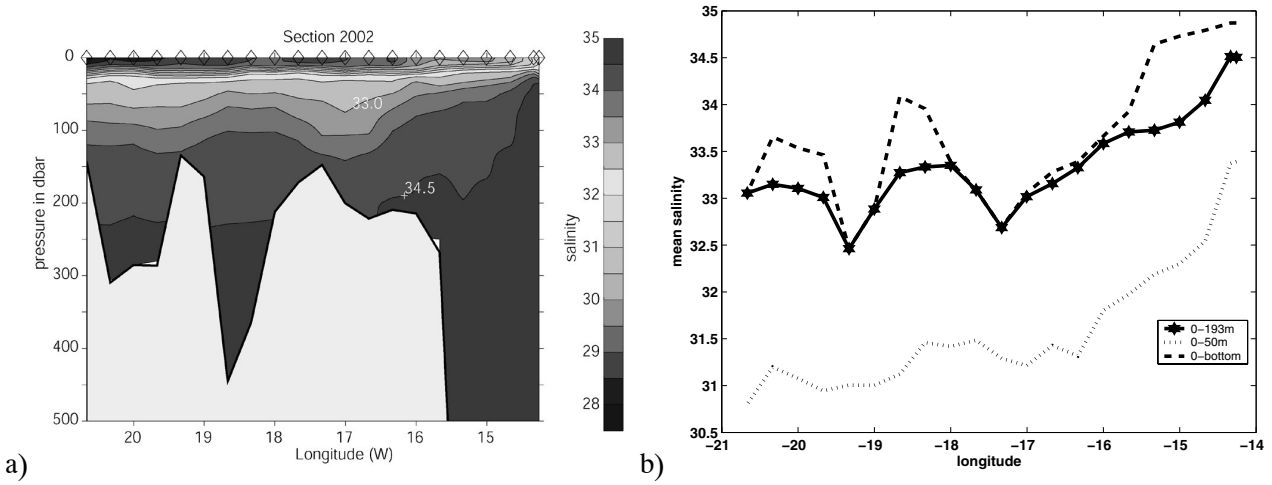

Figure 3: a) Salinity section over the East Greenland shelf at 74°N in September 2002. Station positions are given as rhombi at the surface. b) Vertical mean salinity in different layers from the data in a).

Table 1: Position and instrumentation of the shelf moorings.

Name	Latitude	Longitude	Time	Depth	Instruments
Tube 2	74° 01.624 N	15° 31.230 W	9/2000-9/2001	358 m	Microcat at 41 m and 84 m
Tube 5	74° 01.678 N	15° 31.303 W	9/2001–9/2002	340 m	Microcat at 77 m and 117 m
Tube 6	74° 03.956 N	15° 45.139 W	9/2001–9/2002	203 m	Microcat at 16 m and 56 m
ADCP	74° 02.879 N	15° 38.113 W	9/2001–9/2002	205 m	11 velocity bins
Tube 9	74° 01.656 N	15° 31.289 W	9/2002–10/2003	341 m	Microcat at 15 m and 55 m

major role. Advection of ice from further away would also imply the presence of multi-year ice, but during the years 2000 to 2003 the multi-year ice coverage was only minor. A higher ice cover means also higher salinities, and so in summers in which the ice does not completely melt (e.g. 2000) the salinities are higher than in summers where almost all ice has melted (e.g. 2001, 2002 and 2003). Ice cover gives only the area and not the ice volume, but the observed change in the freshwater content of the water column corresponds to the formation of about 2 m to 2.5 m of ice, being slightly larger then the mean thickness of 1.5 to 2 m of the winter ice drift given by BOURKE and GARRET (1987). Although the mean features of the seasonal cycle are not influenced by advection, some advective events are discernible. Pulses of higher salinity in the lowermost instrument, especially the one at nominal 120 m in 2001–2002, are most probably due to onslope-advection of high salinity recirculating Atlantic Water (rAW). Occasionally higher salinities are seen in the uppermost instruments as a result from a tilting of the mooring in a stronger current, which lowers the instruments to larger depths with higher salinities. No apparent seasonal cycle is found in the mean velocity from the bottom till near the surface. Only the uppermost velocity bin shows a seasonal cycle. The difference between the mean velocity of the lower bins and the uppermost velocity bin is small during winter and larger during summer. Without ice cover the wind forcing of the upper layer is stronger and the density contrast between surface and deeper parts of the water column decouples the surface layer from the underlying layers in summer.

4 The freshwater transport

The freshwater transport (FW) by the EGC is calculated by integrating the product of velocity (v) and salinity-anomaly (observed salinity (S) minus a reference salinity (S_{ref})) over the current width (from x_0 to x_1) and depth (from z_0 to z_1):

$$FW(t) = \int\int v(x,y,t) \times (S(x,y,t) - S_{ref})\, \partial z \partial x$$

S_{ref} is a climatological mean value for the water masses representing the larger scale circulation regime of the Nordic Seas. Here we apply the commonly used reference of 34.9 (e.g. AAGAARD and CARMACK, 1989). For the transport calculation we are using the daily mean values of the salinity and velocity, thus giving us daily transport values for the period in which tube and ADCP data are available (from September 2001 to September 2002). In this period data from two tubes is available. The upper instrument of one tube was situated deeper than the lower instrument of the other mooring. The moorings were placed only 8 km apart and as we have

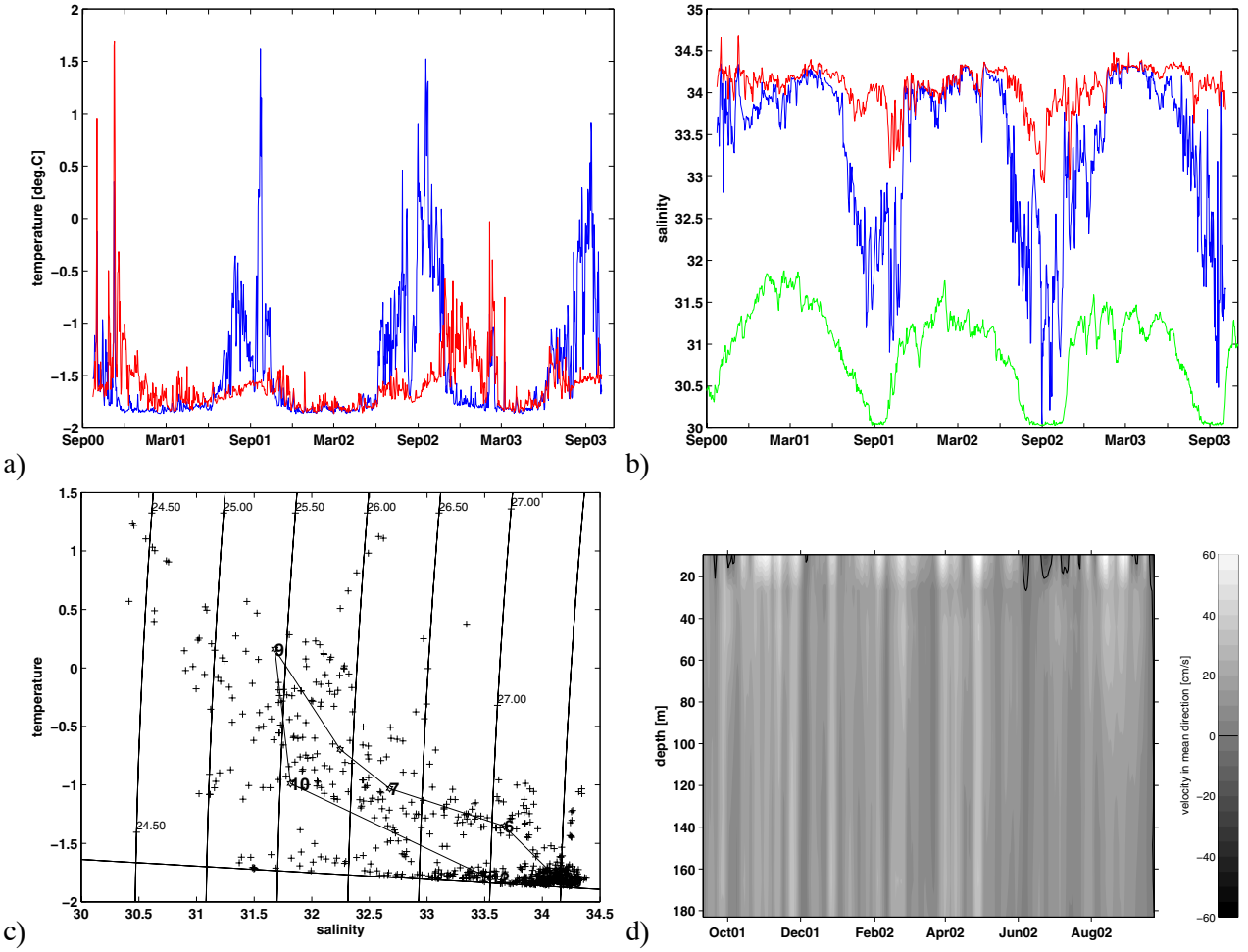

Figure 4: Time series from the period 9/2000 to 9/2003 of a) the temperature at the upper (blue, nominal depth 20 m) and lower (red, nominal depth 60 m) instrument, b) the upper (blue) and lower (red) salinity together with sea ice cover from satellite data (green, 19°W-14°W and 74.0°N-74.5°N, scaled so that 0 % at 30 PSU, 100 % at 32 PSU), c) temperature-salinity data from 4a), b) at the nominal depth of 20 m (+) plotted in temperature/salinity-space, and their 3-year monthly means (red line). Freezing temperature and densities (sigma-theta) are inserted, d) current speed in direction of the mean barotropic flow (225 degrees). All mooring data are daily averages. The velocities in d) are low pass filtered with a cutoff period of 28 hours and a 6 days running mean was applied to suppress shorter term barotropic fluctuations and enhance the baroclinic structure.

Table 2: Estimates of freshwater transport from different data sources.

	Velocity data	**Salinity data**	**Freshwater transport**	**expl.variance. daily**	**expl.variance 15 days mean**
"full"	$u(z,t)$	$S(z,t)$	869	100 %	100 %
"constant"	$\langle\overline{u}\rangle$	$\langle\overline{S}\rangle$	808	0 %	0 %
"barotropic"	$\overline{u}(t)$	$\overline{S}(t)$	804	85 %	92 %
"S-variable"	$\langle\overline{u}\rangle$	$\overline{S}(t)$	808	16 %	54 %
"U-variable"	$\overline{u}(t)$	$\langle\overline{S}\rangle$	808	55 %	37 %
"baroclinic"	$\langle u\rangle(z)$	$\langle S\rangle(z)$	879	0 %	0 %
"total mooring"	$u(z,t)$	mooring summer data	1283	–	–
"total shelf"	$u(z,t)$	CTD summer data	1741	–	–

to assume horizontal homogeneity in the transport calculations (see below) we merged them into a single time series of vertical stratification.

The vertical integral $\int_{z_0}^{z_1} \partial z$ is substituted by the sum $\sum_{z_0}^{z_1} \Delta z$ over the ADCP velocity bins ($\Delta z \sim 17.4$ m) ranging from the surface ($z_0 = 0$ m) to the bottom ($z_1 = 193$ m) at the ADCP position. The salinity data is linearly interpolated onto the respective ADCP depths using the tube measurements and a linear extrapolation to the surface. The extrapolation towards the bottom is to-

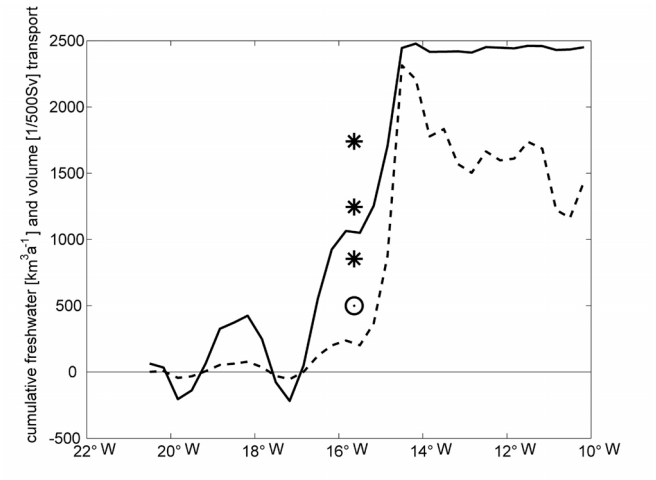

Figure 5: Cumulative (from the west) freshwater (solid) and volume (dashed) transport from geostrophic calculation with a reference velocity of zero at the bottom from the 2002 CTD section along 74°N. The easternmost value is the total geostrophic transport on the shelf and within the EGC. Stars denote the mean freshwater transport estimates from the mooring ("full'", "total mooring" and "total shelf"; see Table 2). The circle denotes the mooring volume transport.

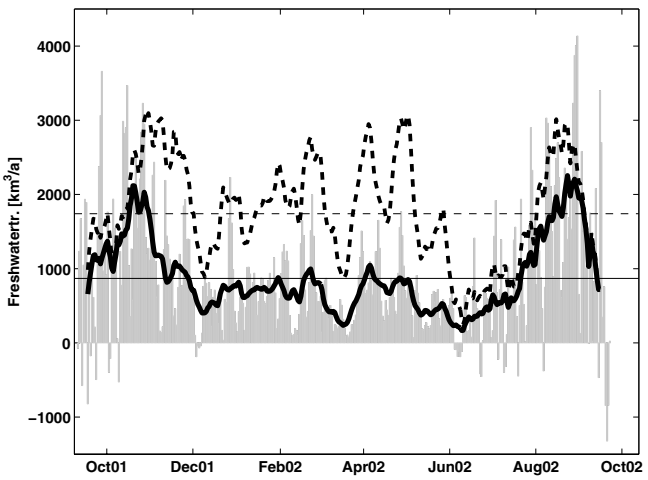

Figure 6: Instantaneous (grey bars) and smoothed (15 days running mean, thick line) freshwater transport in liquid form and the smoothed total transport as calculated using the mean summer salinity profile from CTD data (dashed thick line). The two horizontal lines give the respective mean values (869 and 1741).

wards the deepest summer 2002 CTD salinity value or to the deepest tube measurements if this value is larger then the CTD value. The integration depth of 193 m is quite representative for the whole shelf (see Figs. 1 and 3). Some deeper channels cut into the shelf at 74°N, but since they are dead ends, the transports at these deep levels will be small. As we have only one measurement location we have to assume horizontal homogeneity and can substitute the horizontal integral $\int \partial x$ with a multiplication by the current width (W$= |x_1 - x_0|$). We can make an estimate of the error due to the assumption of homogeneity in salinity using the summer 2002 CTD section which covers the whole shelf. The vertically integrated salinity (0–193 dbar, Fig. 3b) ranges from 32.80 to 33.77. The difference of the vertically integrated salinities at the ADCP position (S=33.69) across the whole shelf (20.5°W to 15°W, S$=$ 33.27) corresponds to a change of 30 % in (S-S$_{ref}$), and the freshwater transport acordingly. As the mean shelf salinity is lower than the mean salinity at the mooring position, our transport underestimates the absolute value of the freshwater transport.

The representativity of the current measurements is more uncertain. The shelf at 74°N is about 150 km wide, too much to assume horizontal homogeneity in the view of possible recirculations or gradients in conditions of a partly ice-covered shelf. From the summer CTD sections we can calculate only the velocity referenced to an assumed level of known motion. ADCP sections are also just snapshots and must be detided, and tidal models are probably very uncertain in this shallow and remote area. Altimetry, even if assuming the errors are small enough to make estimates of the barotropic currents, is also not possible to use, as up till now no oceanic altimetry signal can be measured in ice covered areas. Some information can be deduced from ice drift data (FOWLER, 2003). At the ADCP position the mean southward ice drift (4.6 cm/s) is somewhat smaller then the southward barotropic velocity from the ADCP (6.8 cm/s). The southward ice drift decreases towards the shore, and although ice motion does not depend only on the oceanic surface currents but also on wind and ice compactness it is very probable that the oceanic current speed is also lower towards the coast. Taking the ice drift as proxy for the barotropic velocity the cumulative volume transport (0–193 m, starting at the coast) is 0.8 Sv at the ADCP position and 1.3 Sv at 14°W (1 Sverdrup $= 10^6$ m^3/s). Similar values are found in the geostrophic estimate from CTD data (Fig. 5). If the ice drift underestimates the barotropic current by the same factor as at the ADCP position, the transport at 14°W would increase to 1.9 Sv. We choose the relevant width of the EGC such that the mean total volume transport calculated from the ADCP data amounts to 1 Sv. This leads to an effective width of about 32.1 km using the velocity in the main current direction or of 76.0 km for the north-south component. With all the assumptions going into this fixed current width estimate the errors are large. Certainly further direct current measurements are needed to better estimate the net transport over the shelf. We also do not know if the small horizontal variability of the salinity as seen in the CTD-sections in summer is valid in other seasons.

Fig. 6 shows the time series of the freshwater transport in main current direction calculated from the ADCP

velocities and the mooring salinities. The temporal mean amounts to 869 km^3/a (or 0.027 Sv). To separate the main factors leading to the observed freshwater transport, calculations were done also using different combinations of temporal means ($\langle x \rangle$) and vertical means ($\overline{x}$) of the salinity and velocity (Tab.2). For the temporal mean freshwater transport it suffices to know the temporal and vertical mean values of the velocity and salinity, as the "constant" calculation using $\langle \overline{u} \rangle$ and $\langle \overline{S} \rangle$ gives almost the same value as the full calculation. The "barotropic" calculation also captures most of the temporal variability. A large part of the shorter term variability is due to the current variability (calculation "U-variable") but for the smoothed transport and the main seasonal signal the variability in the salinity is more important (calculation "S-variable"). The main features in the seasonal cycle of the liquid freshwater transport in Fig. 6 are the low values in winter due to the higher winter salinity and and higher values in summer due to the lower summer salinities.

Calculations were also done using just the summer salinity values from the moorings, respective the mean summer salinity profile from the CTD sections. As in the summers no ice was present, the summer transport is equal to the total freshwater transport. With the presence of ice, we have to add the freshwater transport in the form of ice to arrive at the total transport. We found that the seasonal cycle in salinity can be explained quite well with local formation and melting of ice. This means the total freshwater content of the water column stays constant during the year. Assuming, that the ice moves similarly to the water in the upper water column, we can estimate the total transport by multiplying the measured velocities with the mean salinity profile in summer. The total freshwater transport is about 1250 to 1750 km^3/a, the transport in the form of ice being as large as the transport in liquid form. Comparing our estimate with the total fresh water flux trough Fram Strait, our value is very low and a better fit would be attained using a volume transport of 2 Sv in the current width calculation. The seasonal cycle of the ice transport is opposed to the seasonal cycle of the liquid freshwater transport, with a maximum in winter and a minimum in summer (and equal zero during ice free summers). This also corresponds to the seasonal cycle of the ice transport in Fram Strait (VINJE, 2001), with the difference that in Fram Strait the summer ice export does not reach a value of zero due to the year-round presence of ice.

5 Conclusions

We have demonstrated in this paper that time series of temperature, salinity and currents can successfully be obtained in the upper layers of the seasonally ice-covered waters of the East Greenland shelf. These data were used to estimate the seasonal variability of the liquid fraction of the freshwater transport of the EGC. The simple instrumentation proved rugged enough to be employed in future monitoring of the Arctic freshwater export which is an essential component in all planning for improved estimates on the global freshwater cycle. However, a full transport monitoring of the EGC needs additional steps to be taken:

– In order to gain information on the divergence of the EGC-freshwater flux, measurement array need to be maintained between Fram Strait and south of the Denmark Strait at those locations, where topography forces injections of freshwater into the interior of the Nordic and the Labrador Seas. This information is vital in estimating the individual contributions of the convective gyres to the dense overflows.

– The number of instruments covering individual sections across the East Greenland shelf and upper slope has to be large enough to allow reliable interpolation of the salinity and velocity fields.

– The measurements of liquid freshwater fluxes are of minor value if not the information on freshwater fluxes with the ice is available in parallel. Here we expect major improvements once the thickness of the sea ice is routinely available from satellites like CryoSat and IceSat.

Acknowledgements

The contributions by Gunda WIECZOREK and John MORTENSEN to field work and data analysis are acknowledged. So are the technical skills of Ulrich DRUEBBISCH, Andreas WELSCH and Helmuth WUELLNER who took great care to provide moorings which survive the harsh conditions of the East Greenland shelf. The work was funded by the DFG-Sonderforschungsbereich 512 (Teilprojekte C4, E2) and by the University of Hamburg. It also profitted from the parallel activities at 63°N, funded under EU-FP 5 contract EVK2-CT2002-0149ASOF-W

References

AAGAARD, K., E. C. CARMACK, 1989: The role of sea ice and other freshwater in the Arctic circulation. – J. Geophys. Res. **94**(14), 14,485–14,498.

BLINDHEIM, J.,V. BOROKOV, B. HANSEN, S.-A. MALMBERG, W.R. TURRELL, S. OESTERHUS, 2000: Upperlayer cooling and freshening in the Norwegian Sea in relation to atmospheric forcing. – Deep-Sea Research I **47**, 655–680.

BOURKE, R.H., R.P. GARRET, 1987: Sea ice thickness distribution in the Arctic Ocean. – Cold Regions Sci. Technol. **13**, 259–280.

DEWEY, R., MOORING DESIGN & DYNAMICS A MATLAB®, 1991: Package for Designing and Analyzing Oceanographic Moorings and Towed Bodies. – Marine Models, Online Vol (**1**), 103–157.

DICKSON, R.R., I. YASHAYAEV, J. MEINCKE, W.R. TURRELL, S. DYE, J. HOLFORT, 2002: Rapid freshening of the deep North Atlantic over the past four decades. – Nature **426**, 826–829.

FOWLER, C., 2003: Polar Pathfinder Daily 25 km EASE-Grid Sea Ice Motion Vectors. – Boulder, CO, USA: National Snow and Ice Data Center. Digital media.

HAAK, H., J. JUNGCLAUS, U. MIKOLAJEWICZ, M. LATIF, 2003: Formation and propagation of great salinity anomalies. – Geophys. Res. Letters **30**(9), 1473, 1–4.

HAEKKINEN, S., 1999: A Simulation of a Great Salinity Anomaly. – J. Climate **12**, 1781–1795.

HANSEN, B., W.R. TURELL, S. ØSTERHUS, 2001: Decreasing overflow from the Nordic seas into the Atlantic Ocean through the Farce-Shetland Channel since 1950. – Nature **411**, 927–930.

HARDER, M., P. LEMBKE, M. HILMER, 1998: Simulation of sea ice transport through Fram Strait: Natural Variability and sensitivity to forcing. – J. Geophys. Res. **103** (C3), 5595–5606.

HILMER, M., M. HARDER, P. LEMKE, 1998: Sea ice transport: a highly variable link between Arctic and North Atlantic. – Geophys. Res. Letters **26**(17), 3359–3362.

IOC, IHO, BODC, 2003: Centenary Edition of the GEBCO Digital Atlas. – Published on CD-ROM on behalf of the Intergovernmental Oceanographic Commission and the International Hydrographic Organization as part of the General Bathymetric Chart of the Oceans, British Oceanographic Data Centre, Liverpool, U.K.

KÖBERLE, C., R. GERDES, 2003: Mechanisms determining the variability of Arctic sea ice conditions and export. – J. Climate **16**, 2843–2858.

KWOK, R., D.A. ROTHROCK, 1999: Variability of Fram Strait ice flux and the North Atlantic Oscillation. – J. Geophys. Res. **104**, 5177–5189.

MEREDITH, M., K. HEYWOOD, P. DENNIS, L. GOLDSON, R. WHITE, E. FAHRBACH, U. SCHAUER, S. OSTERHUS, 2001: Freshwater fluxes through the western Fram Strait. – Geophys. Res. Letters **28**(8), 1615–1618.

PROUDMAN, J., 1953: Dynamical Oceanography. – Methuen, London and Wiley, New York, 409 pp.

RUDELS, B., 1987: On the mass balance of the Polar Ocean, with special emphasis on the Fram Strait. – North Polarinstitutt Skrifter **188**, 53 pp.

RUDELS, B., E. FAHRBACH, J. MEINCKE, G. BUDEUS, P. ERIKSSON, 2002: The East Greenland Current and its contribution to the Denmark Strait overflow. – ICES Journal of Marine Sciences **59**, 1133–1154.

VINJE, T., 2001: Fram strait Ice fluxes and atmospheric circulation 1950–2000. – J. Climate **14**, 3508–3517.

VINJE, T., N. NORDLUND, A. KVAMBEK, 1998: Monitoring ice thickness in Fram Strait. – J. Geophys. Res. **103**(10), 10,437–10,449.